A Novel Feeding Network for Sequential Rotation Array Antennas Above the Ground Plane

Kazuhide Hirose, Naonoshin Ito, Yuya Urushibata, and Hisamatsu Nakano

Abstract – We propose a coplanar feeding network for array antennas using the moment method. A one-wavelength loop feeds four spiral elements sequentially rotated by 90°. The loop points at a quarter wavelength apart are excited either directly or via two straight wires vertical to the ground plane. The antennas with and without the straight wires show a 3 dB axial ratio bandwidth of 51% and a constant axial ratio of 0 dB, respectively. Subsequently, the straight wires are replaced with a branched wire to create a simple antenna feeding system. Numerically and experimentally, the antenna has an axial ratio bandwidth of 39%, which is wider than the isolated spiral element by a factor of 1.6.

1. Introduction

A sequential rotation (SR) technique expands the axial ratio bandwidth of a circularly polarized (CP) array antenna [1–3]. In the array, the radiation elements are sequentially rotated and excited by a sequential feeding network. Various types of feeding networks have been investigated, including groove gap waveguides [1], rectangular back cavities [2], and microstrip lines [3].

This study proposes a novel sequential feeding network for a CP array antenna above the ground plane. A coplanar one-wavelength loop is used to feed four spiral elements that are sequentially rotated by 90°. The antenna is analyzed using the moment method [4], where the spiral height above the ground plane is taken to be a quarter wavelength [5].

The motivation for using a one-wavelength loop as a feeding network is based on the following facts: 1) A type of horizontal half-wavelength dipole at a quarter wavelength above the ground plane operates as a coplanar feeding network for an array antenna [6]. 2) A type of vertical quarter-wavelength monopole on the ground plane operates as a feeding network for a CP antenna [7]. These facts encourage the expectation of a type of horizontal one-wavelength loop at a quarter wavelength above the ground plane to operate as a coplanar feeding network for a sequentially rotated antenna array.

This study first analyzes a reference antenna with a loop of two balanced sources (see Figure 1a). Next, the balanced sources are transformed into unbalanced ones using straight vertical wires (see Figure 1b). Finally, the two unbalanced sources are reduced to one source for a simple feeding system.

Manuscript received 18 October 2023.

Kazuhide Hirose, Naonoshin Ito, and Yuya Urushibata are with the College of Engineering, Shibaura Institute of Technology, Tokyo 135-8548, Japan; email: khirose@sic.shibaura-it.ac.jp; ma21015@shibaura-it.ac.jp; ma23028@shibaura-it.ac.jp.

Hisamatsu Nakano is with the Science and Engineering, Hosei University, Tokyo 184-8584, Japan; e-mail: hymat@hosei.ac.jp.

2. Reference and Present Antennas With Two Sources

Figure 1 shows the antenna configurations. Each antenna is located above the ground plane at height h. Four spiral elements are sequentially rotated by 90° and connected to a coplanar loop of circumference C_L via segments of length L_c. The spiral element is specified by circumference C_S, adjacent arm distance d, and straight-line length L_s, as shown in Figure 1a. The antenna is made of wires of radius ρ [5–7].

The loop of the reference antenna is excited by two delta gap generators (balanced sources) at points F_n ($n = 1$ and 2), located at $\phi = \pm 45°$. In contrast, the loop points F_n of the present antenna are connected to vertical straight wires F_n–F_n' of radius ρ, and the bottom ends F_n' are excited by two coaxial lines (unbalanced sources), as shown in Figure 1b. Note that the two sources have the same amplitudes and a phase difference of 90° for both the present and reference antennas. Also note that the balanced sources are located along the loop arm, as shown in Figure 1a, and each source requires a balun circuit for an experiment using a coaxial line feed, unlike the unbalanced sources, shown in Figure 1b.

The antenna is analyzed using our developed computer program based on the moment method [4],

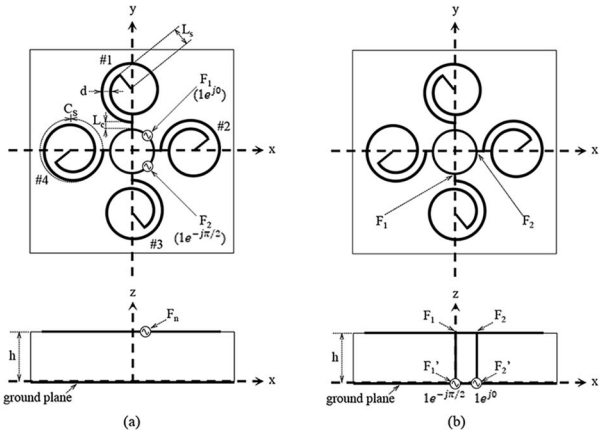

Figure 1. Antenna configurations with two sources. (a) Reference antenna with balanced sources at loop points F_n ($n = 1$ and 2). (b) Present antenna with unbalanced sources at point F_n' using vertical straight wires F_n–F_n'.

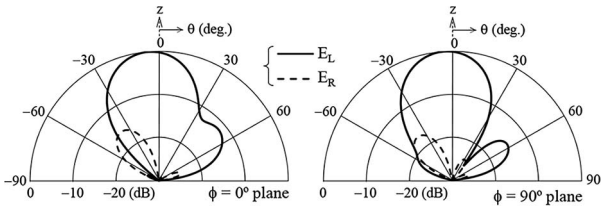

Figure 2. Radiation patterns of a reference antenna.

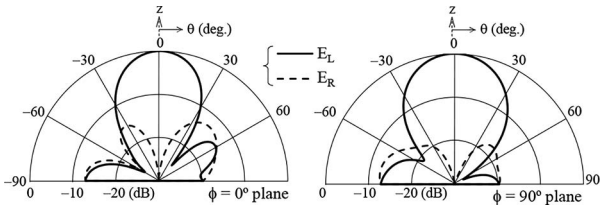

Figure 4. Radiation patterns of a present antenna.

where the ground plane is assumed to be an infinite extent. The loop circumference is taken to be $C_L = 1\lambda_0$, where λ_0 is the free-space wavelength at a test frequency of f_0. The spiral parameters (C_S, d, L_s) and segment length L_c are selected for CP radiation. The other configuration parameters are fixed at the same values (h, ρ) = ($\lambda_0/4$, $\lambda_0/200$) as those in [5–7] throughout this study.

Preliminary calculations reveal that the segment length L_c must be small for CP radiation. The radiation patterns of the reference antenna for $L_c = 0.05\lambda_0$ are shown in Figure 2. The spiral parameters are (C_S, d, L_s) = ($1.46\lambda_0$, $0.062\lambda_0$, $0.145\lambda_0$). The radiation is decomposed into right-hand (E_R) and left-hand (E_L) CP wave components that are shown with dotted and solid lines, respectively. A left-handed CP beam is obtained in the direction normal to the antenna plane in the $+z$-axis direction. The half-power beamwidths (HPBWs) in the $\phi = 0°$ and 90° planes are 35° and 35°, respectively.

The radiation beam normal to the antenna plane is obtained because a coplanar loop has a traveling wave current distribution and operates as a sequential feeding network for the spiral elements. This is shown in Figure 3, where the second row shows the loop current together with spiral ones in the top and bottom rows. It is observed that the phase of the loop current linearly varies along the length, leading to a sequential phase shift of 90°, which is necessary for spiral element excitation. As a result, the spiral elements of one to four have the current phases that are sequentially delayed by 90°. This delay compensates for the phase progress of the partial radiation from each rotated spiral to form the normal beam.

Based on the radiation characteristics of the reference antenna, we analyze the present antenna with the straight wires F_n–F_n'. Figure 4 shows the simulated radiation patterns of the present antenna. The spiral parameters and segment length are identical to those of the reference antenna. It is observed that the CP radiation beams are similar to those of the reference antenna. The HPBWs are 34° and 37° in the $\phi = 0°$ and 90° planes, respectively.

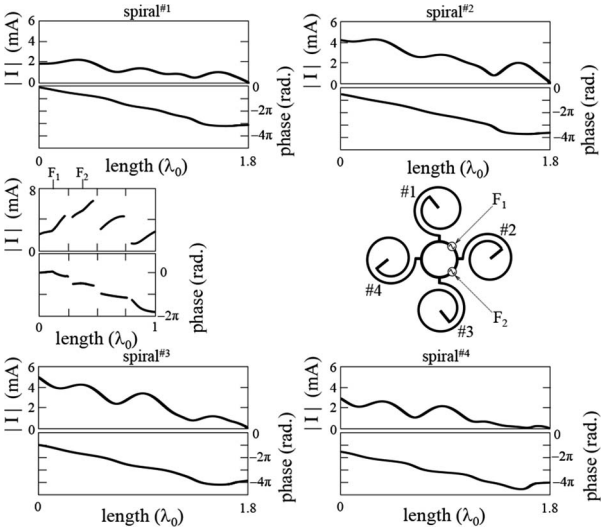

Figure 3. Current distributions of a reference antenna, with |I| denoting the current amplitude.

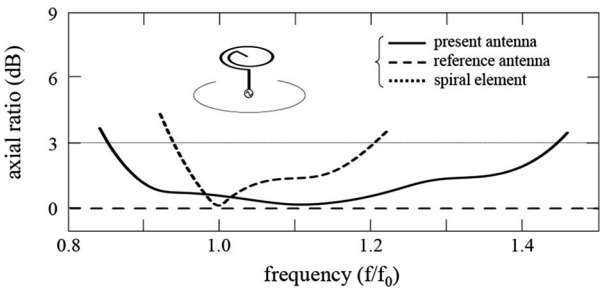

Figure 5. Frequency responses of axial ratio of reference and present antennas, together with a single spiral element.

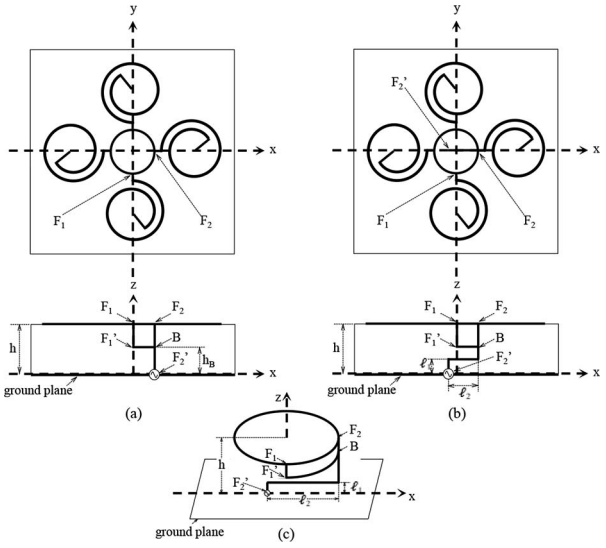

Figure 6. Antenna configurations with one source at point F_2' using a vertical branched wire F_n–B–F_2'. (a) Straight wire B–F_2'. (b) Crank wire B–F_2'. (c) Perspective view of a loop with a crank wire B–F_2'.

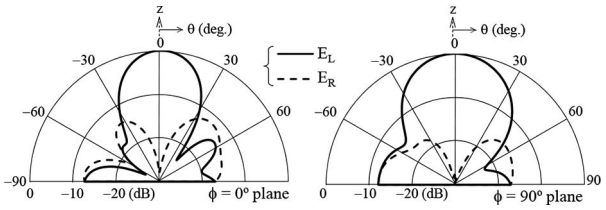

Figure 7. Radiation patterns for a straight wire B–F_2'.

The solid and dashed lines in Figure 5 show the simulated axial ratio versus frequency for the present and reference antennas. It is revealed that the present antenna shows a 3 dB axial ratio bandwidth of 51%, whereas the reference antenna's axial ratio is constant at 0 dB, as expected. For comparison, the dotted line shows the result for an isolated spiral element without an array environment shown in the inset, where the outer arm end of the spiral element at a height of $\lambda_0/4$ above the ground plane is excited by a coaxial line via a vertical wire. It can be said that the bandwidth of the present antenna is twice as wide as that of the spiral element (24%).

3. Antenna With One Source

Thus far, we have investigated an array antenna with two sources. In this section, the double sources are reduced to a single source to simplify the antenna feeding system.

The antenna configuration is shown in Figure 6a. The loop points F_n are connected to a vertical branched wire F_n–B–F_2' of radius ρ, and the bottom end F_2' is excited by one unbalanced source. The branch-point height h_B is selected so that the axial ratio bandwidth

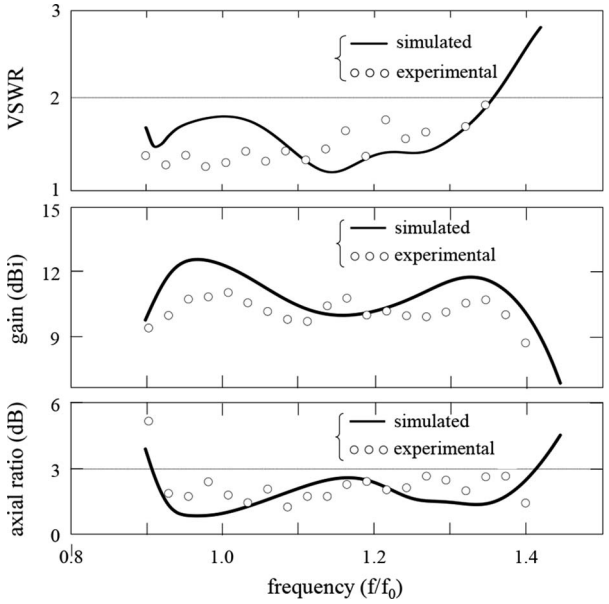

Figure 8. VSWR, axial ratio, and gain versus frequency for a crank wire B–F_2'.

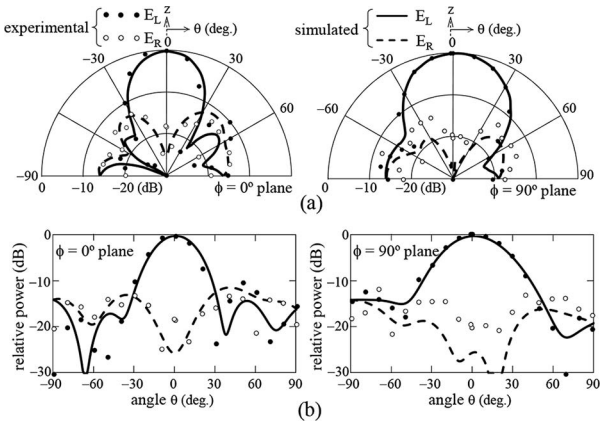

Figure 9. Radiation patterns for a crank wire B–F_2'. (a) Polar coordinates. (b) Rectangular coordinates.

reaches its maximum value. The other configurations are the same as those of the present antenna described in Section 2. Note that a branched wire part F_1'–B has the same arc shape as the coplanar loop part F_1–F_2, as shown in Figure 6c.

The simulated radiation patterns are shown in Figure 7. The branch-point height is $h_B = 0.15\lambda_0$. The antenna radiates a CP beam similar to that of the two sources (see Figure 4). The axial ratio bandwidth is evaluated to be 46%.

Next, consideration is given to input impedance that matches the coaxial line. For this, we transform the straight wire B–F_2' into a crank one, as shown in Figure 6b. We select the crank wire parameters (ℓ_1, ℓ_2) for a voltage standing wave radio (VSWR) of less than two, while fixing the other configuration parameters for the radiation characteristics to remain unchanged.

Calculations show that we must choose the ℓ_1 ($=0.02\lambda_0$) to be as small as possible. The ℓ_2 ($=0.22\lambda_0$) is selected so that the VSWR <2 bandwidth reaches the maximum value. The solid line in Figure 8 shows the simulated VSWR versus frequency, with the axial ratio and gain. The VSWR is evaluated for a 50 Ω coaxial line. The overlap bandwidth of the VSWR <2 and axial ratio <3 dB is 39% (1.6 times as wide as the spiral element), where the gain is more than 10.0 dBi.

The simulated radiation patterns are shown with solid and dotted lines in Figure 9. The CP beams are almost the same as those for the straight wire B–F_2' (see Figure 7).

Figure 10. Photographs of an antenna with a crank wire B–F_2'. (a) Top view. (b) Side view.

Table 1. Comparison with similar studies

Study	Array type	Axial ratio bandwidth (%)	Gain (dBi)	Frequency (GHz)	Radiation element[b]	Sequential rotation[b]	Antenna size $x \times y \times z$ (λ_0^3; z: height)
[1]	4×4	14[a]	19.24	30	P	A	$4.8 \times 4.8 \times 1.7$
[2]	4×4	23.8	20.5	65	P	A	$4.4 \times 8.5 \times 0.5$
[3]	8×8	18.3	18.5	25	P	A	$5.6 \times 5.6 \times 0.09$
[5]	1×7	21	14.5	3	S	NA	$0.9 \times 3.4 \times 0.25$
[9]	$1 \times 8 \times 15$	4	17.7	24	P	A	$17.0 \times 8.0 \times 0.1$
[10]	2×2	20.4	11.1	27	P	A	$2.9 \times 2.9 \times 0.1$
[11]	2×2	18.9	13.8	5.6	P	A	$- \times - \times 0.1$
This study	2×2	39	12.3	3	S	A	$1.4 \times 1.4 \times 0.25$

[a] 1.5 dB axial ratio bandwidth.
[b] P, patch; A, applied; S, spiral; NA, not applied; –, not described.

The HPBWs in the $\phi = 0°$ and 90° planes are 31° and 44°, respectively. The gain is 12.3 dBi.

Up to this point, we have discussed the radiation characteristics using the simulated results. To validate these results, we perform experiments using a fabricated antenna at $f_0 = 3$ GHz, with a ground plane of $5\lambda_0 \times 5\lambda_0$ (50 cm × 50 cm), having an antenna size of 14 cm × 14 cm × 2.5 cm. Photographs of the antenna are shown in Figure 10. The small circles and dots in Figures 8 and 9 show the experimental results. A good agreement is observed between the experimental and simulated results. Note that the antenna's radiation efficiency is theoretically almost 100% because only the conductor losses are negligible up to a 12 GHz band [8].

Finally, we compare the results for a crank wire B–F_2' with those of other similar studies. Table 1 summarizes these comparisons. Note that we realize the widest axial ratio bandwidth using a coplanar one-wavelength loop as a sequential feeding network. Also note that a previous study [5] discussed a spiral antenna array without SR, resulting in an axial ratio bandwidth of 21%, which was lower than our result.

Before concluding, we mention an array factor with degree. The array degree is four because the array consists of one loop and four spirals. The array factor may be determined using $P_n(x, y)$ with $E_n(A, \Phi)$, where P_n with E_n are the nth element position with the excitation amplitude A and phase Φ. Each spiral position A is evaluated using the input current amplitude at each leftmost in the abscissa shown in Figure 3, and the loop position A corresponds to the average current amplitude along the loop. All the spiral positions have the same phase, nearly equal to the loop position Φ, due to the beam formation in the direction normal to the antenna plane.

4. Conclusion

We have studied two array antennas, each having a coplanar loop with two balanced or unbalanced sources. The balanced and unbalanced source antennas exhibited a constant axial ratio of 0 dB and a 3 dB axial ratio bandwidth of 51%, respectively. Subsequently, the two unbalanced sources are reduced to one source using a branched wire vertical to the ground plane. Numerically and experimentally, the axial ratio bandwidth is 39%, where the gain and VSWR are more than 10.0 dBi and less than 2.

5. Acknowledgments

The authors thank Wiley's English language service and Lisa Patel for assistance in preparing this manuscript.

6. References

1. M. F. Rocher, J. H. Herruzo, A. V. Nogueira, and B. B. Clemente, "Single-Layer Sequential Rotation Network in Gap Waveguide for a Wideband Low-Profile Circularly Polarized Array Antenna," *IEEE Access*, **10**, June 2022, pp. 62157-62163.
2. Z. Qi, Y. Zhu, and X. Li, "Compact Wideband Circularly Polarized Patch Antenna Array Using Self-Sequential Rotation Technology," *IEEE Antennas and Wireless Propagation Letters*, **21**, 4, April 2022, pp. 700-704.
3. R. Ma, Z. Jiang, Y. Zhang, X. Wu, T. Yue. et al., "Theory, Design, and Verification of Dual-Circularly Polarized Dual-Beam Arrays With Independent Control of Polarization: A Generalization of Sequential Rotation Arrays," *IEEE Transactions on Antennas and Propagation*, **69**, 3, March 2021, pp. 1369-1382.
4. R. F. Harrington, *Fields Computation by Moment Methods*, New York, Macmillan, 1968.
5. K. Hirose, Y. Tamura, M. Tsugane, and H. Nakano, "Coplanar Series-Fed Spiral Antenna Arrays for Enlarged Axial Ratio Bandwidth," *Progress in Electromagnetics Research Letters*, **108**, November 2022, pp. 1-8.
6. K. Hirose, Y. Kikkawa, and H. Nakano, "Decoupling and Sequential Array Antennas—Effects of Coplanar Feedline on Radiation Characteristics," *IEEE Antennas and Wireless Propagation Letters*, **19**, 3, March 2020, pp. 423-427.
7. K. Hirose, S. Tsubouchi, and H. Nakano, "A Loop Antenna With Quasi-Two Sources for Circular Polarisation," *Electronics Letters*, **58**, 6, March 2022, pp. 222-224.
8. H. Nakano, T. Oka, K. Hirose, and J. Yamauchi, "Analysis and Measurements for Improved Crank-Line Antennas," *IEEE Transactions on Antennas and Propagation*, **45**, 7, July 1997, pp. 1166-1172.
9. Y. Cao, S. Yan, J. Li, and J. Chen, "A Pillbox Based Dual Circularly-Polarized Millimeter-Wave Multi-Beam

Antenna for Future Vehicular Radar Application," *IEEE Transactions on Vehicular Technology*, **71**, 7, July 2022, pp. 7095-7103.

10. M. Sun, N. Liu, L. Zhu, and G. Fu, "Wideband Circularly Polarized Sequentially Rotated Microstrip Antenna Array With Sequential-Phase Feeding Network," *Journal of Communications and Information Networks*, **5**, 3, March 2020, pp. 350-357.
11. N. Yan, K. Ma, and Y. Luo, "An SISL Sequentially Rotated Feeding Circularly Polarized Stacked Patch Antenna Array," *IEEE Transactions on Antennas and Propagation*, **68**, 3, July 2020, pp. 2060-2067.